JOC Article

Conformation of the Galactose Ring Adopted in Solution and in Crystalline Form as Determined by Experimental and DFT ^{1}H NMR and Single-Crystal X-ray Analysis

Mattias U. Roslund,*[,†,‡] Karel D. Klika,*[,§] Reko L. Lehtilä,[†,‡] Petri Tähtinen,[§] Reijo Sillanpää,[||] and Reko Leino[†,‡]

Department of Organic Chemistry, Åbo Akademi University, Biskopsgatan 8, FIN-20500 Åbo, Finland, Biotie Therapies Corp., Viikinkaari 9, FIN-00710 Helsinki, Finland, Structural Chemistry Group, Department of Chemistry, University of Turku, Vatselankatu 2, FIN-20014 Turku, Finland, and Department of Chemistry, University of Jyväskylä, Survontie 9, FIN-40014 Jyväskylä, Finland

mattias.roslund@abo.fi; karel.klika@utu.fi

Received September 24, 2003

The solution-state conformations of various galactose derivatives were determined by comparison of the experimental ^{1}H−^{1}H vicinal coupling constants to those calculated using density functional theory (DFT) at the B3LYP/cc-pVTZ//B3LYP/6-31G(d,p) level of theory. The agreement between the experimental and calculated vicinal coupling constants for 1,2:3,4-di-*O*-isopropylidene-α-D-galactopyranose was good, thereby confirming an $^OS_2$ skew conformation for it and its derivatives on the basis of their similar observed couplings. Single-crystal X-ray analysis of 1,2:3,4-di-*O*-isopropylidene-6-*O*-(3,4,6-tri-*O*-acetyl-2-deoxy-2-*N*-phthalimido-*β*-D-glucopyranosyl)-α-D-galactopyranose and 1,2,3,4,6-penta-*O*-acetyl-α-D-galactopyranose provided $^OS_2$ and $^4C_1$ conformations, respectively, for the galactose ring in the solid state. The solid-state structures proved to be suitable starting structures for further DFT structure refinement or for immediate calculation of the coupling constants.

Introduction

Carbohydrates occur widely in all living matter and function as structural or protective materials, as energy stores, and even appear to be essential to the process of infection by certain pathogenic species; as such, they have a significant biological role.[1] The conformational analysis of carbohydrates, and in particular, the ring conformation, is of interest as biological activities, as well as chemical and physical properties, are determined to various degrees by the adopted conformations of the substrates.[2] The conformation adopted by a sugar ring, however, can change markedly upon derivatization. For example, the isopropylidene acetal group is a common protecting group widely used[3] in carbohydrate chemistry for 1,2-diols and when applied to D-galactose (**1**), the formation of 1,2:3,4-di-*O*-isopropylidene-α-D-galactopyranose (**2**) is known to change the preferred conformation of the galactose ring in **1** from a $^4C_1$ chair conformer to a skew[4] (twist-boat) conformer;[5] even formation of a 1,2-*O*-isopropylidene or 3,4-*O*-isopropylidene derivative results in a conformational mixture consisting of chair and skew conformers for the product.[5b] These structural changes are evidenced by the ^{1}H−^{1}H vicinal coupling constants ($^3J_{H,H}$) of the ring protons in these compounds as well as by their altered reactivities. It is widely accepted that the ring conformation can readily be ascertained by application of the Karplus equation,[6] and although the Karplus relationship has stood up well for almost half a century, there are problems associated[7−12] with the method, viz. obtaining good values for the constants[8,10,12,13] in the particular variant of the equa-

* Corresponding authors. (M.U.R.) Phone: 358-(2)-2154501. Fax: 358-(2)-2154866. (K.D.K.) Phone: 358-(2)-3336762. Fax: 358-(2)-3336700.
† Åbo Akademi University.
‡ Biotie Therapies Corp.
§ University of Turku.
|| University of Jyväskylä.

(1) (a) Dwek, R. A. *Chem. Rev.* **1996**, *96*, 683−720. (b) *Essentials of Glycobiology*; Varki, A., Cummings, R., Esko, J., Freeze, H., Hart, G., Marth, J., Eds.; Cold Spring Harbor Laboratory Press: Cold Spring Harbor, NY, 1999.
(2) James, L. C.; Roversi, P.; Tawfik, D. S. *Science* **2003**, *299*, 1362−1367.
(3) (a) Rauter, A. P.; Ramôa-Ribeiro, F.; Fernandes, A. C.; Figueiredo, J. A. *Tetrahedron* **1995**, *51*, 6529−6540 and references therein. (b) Clode, D. M. *Chem. Rev.* **1979**, *79*, 491−513.
(4) According to IUPAC nomenclature. McNaught, A. D. *Pure Appl. Chem.* **1996**, *68*, 1919−2008.
(5) (a) Cone, C.; Hough, L. *Carbohydr. Res.* **1965**, *1*, 1−9. (b) Midland, M. M.; Asirwatham, G.; Cheng, J. G.; Miller, J. A.; Morell, L. A. *J. Org. Chem.* **1994**, *59*, 4438−4442.
(6) (a) Karplus, M. *J. Am. Chem. Soc.* **1963**, *85*, 2870−2871. (b) Karplus, M. *J. Chem. Phys.* **1959**, *30*, 11−15. (c) Karplus, M. *J. Phys. Chem.* **1960**, *64*, 1793−1798.
(7) Buys, H. R. *Recueil* **1969**, *88*, 1003−1011.
(8) Haasnoot, C. A. G.; de Leeuw, F. A. A. M.; Altona, C. *Tetrahedron* **1980**, *36*, 2783−2792.
(9) (a) Lambert, J. B. *Acc. Chem. Res.* **1971**, *4*, 87−93. (b) Lambert, J. B.; Papay, J. J.; Khan, S. A.; Kappauf, K. A.; Magyar, E. S. *J. Am. Chem. Soc.* **1974**, *96*, 6112−6118. (c) Lambert, J. B.; Sun, H.-N. *Org. Magn. Reson.* **1977**, *9*, 621−626.
(10) Aliev, A. É.; Sinitsyna, A. A. *Bull. Russ. Acad. Sci.—Div. Chem. Sci.* **1992**, *41*, 1143−1160.
(11) Haasnoot, C. A. G. *J. Am. Chem. Soc.* **1993**, *115*, 1460−1468.
(12) (a) Wu, A.; Cremer, D. *J. Phys. Chem. A* **2003**, *107*, 1797−1810. (b) Wu, A.; Cremer, D.; Auer, A. A.; Gauss, J. *J. Phys. Chem. A* **2002**, *106*, 657−667.

10.1021/jo035400u CCC: $27.50
Published on Web 12/11/2003

tion that is to be applied. There are a number of factors,[6a,9,10,13−15] aside from the torsion angle, such as substituent effects (electronegativity of the substituents), steric and stereoelectronic factors, hybridization states, interceding bond angles and lengths, torsional vibrations, and even solvent effects, etc., that influence the magnitude of $^3J_{H,H}$. Indeed, for each vicinal pair of protons in a set molecule, a different set of constants can be considered to be in effect, rendering the approach laborious and overly complicated even for small molecules where a conformation might nevertheless be defined by a relatively small number of coupling constants, such as the conformation of a sugar ring. Thus, the results can be misleading despite quality attempts[8] to surmount the problem by uniquely defining for each vicinal pair a set of appropriate constants, wherein the problem quickly becomes complex and the exercise self-defeating.

A conformational re-examination of **2**, together with the analogous compounds 1,2:3,4-di-*O*-isopropylidene-6-*O*-(3,4,6-tri-*O*-acetyl-2-deoxy-2-*N*-phthalimido-*β*-D-glucopyranosyl)-α-D-galactopyranose (**3**) and 1,2:3,4-di-*O*-isopropylidene-6-*O*-*tert*-butyldiphenylsilyl-α-D-galactopyranose (**4**), was considered worthwhile, as there has been some doubt and confusion[5a] regarding the conformation of **2**. In this study, we desired to either confirm the proposed $^OS_2$ conformer as the dominant conformer for **2**−**4** or assess the system as a confluence of contributing conformers (i.e., a dynamic equilibrium). A dynamic conformational equilibrium is not unexpected given that the energy barrier for pseudorotation can be very low. It was necessary, therefore, not only to identify the particular skew form(s) by reliably extracting the $J_{H,H}$s but also to apply a methodology that could faithfully guarantee the provision of accurate $J_{H,H}$s. A recent methodology that has been developed[16] and applied[17] to conformational analysis is the calculation of $J_{H,H}$s using density functional theory (DFT). One important criterion for success, however, is the need for good geometry optimization, and for this structures obtained from X-ray analysis were used directly for calculation of the coupling constants as well as for initial starting structures for further DFT geometry optimization.

Results and Discussion

The synthesis of the known compounds **2**,[3a,18] **3**,[18f,19] and **4**,[20] followed literature methodology or standard procedures (Scheme 1). In the case of the protected disaccharide **3**, an important building block for certain biologically significant oligosaccharides, an altered procedure was applied. The introduction of isopropylidene groups to produce **2** from D-galactose (**1**), however, can be accomplished by a number of methods: homogeneously using dry acetone and acid[18b,21] or a Lewis acid catalyst such as zinc chloride;[22] heterogeneously using acetone and Dowex[23] or Amberlyst ion-exchange resins,[24] zeolite catalysts,[3a] or montmorillonite clay;[18e] or by acid-catalyzed transacetalization using an appropriate iso-

SCHEME 1. Reaction Sequences Leading to Compounds 2−4 Examined in This Study[a]

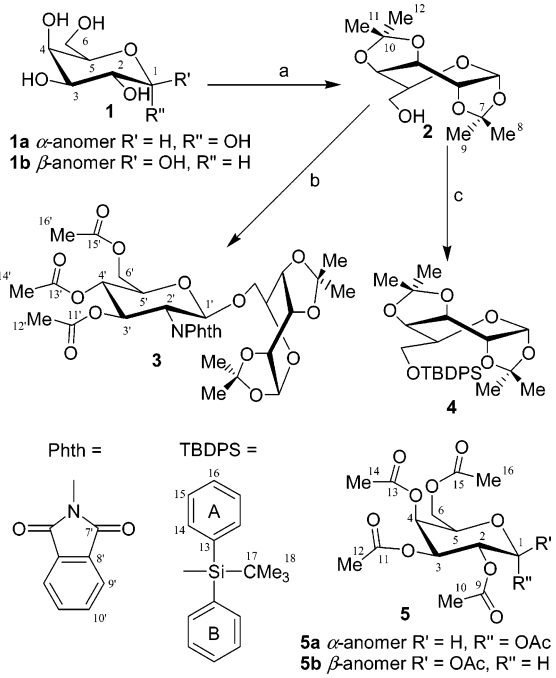

[a] The $^4C_1$ conformation adopted by both α- and β-D-galactose (**1a** and **1b**) is altered to an $^OS_2$ skew conformation in compounds **2**−**4**. The numbering system in use for compounds **1**−**5** is also indicated. Legend: (a) $CuSO_4$, H_2SO_4, acetone, 24 h, rt, 95%; (b) 3,4,6-tri-*O*-acetyl-2-deoxy-2-*N*-phthalimido-α-D-bromoglucose, together with 2,2,6,6-tetramethylpiperidine, 4 Å molecular sieves, and AgOTf, 5 h, −50 to 0 °C, 70%; (c) TBDPSCl, DBU, 17 h, 0 °C to room temperature, 82%.

(13) (a) Ōsawa, E.; Ouchi, T.; Saito, N.; Yamato, M.; Lee, O. S.; Seo, M.-K. *Magn. Reson. Chem.* **1992**, *30*, 1104−1110. (b) Barfield, M.; Smith, W. B. *J. Am. Chem. Soc.* **1992**, *114*, 1574−1581. (c) Smith, W. B.; Barfield, M. *Magn. Reson. Chem.* **1993**, *31*, 696−697. (d) Smith, W. B.; Barfield, M. *Magn. Reson. Chem.* **1996**, *34*, 740. (e) Altona, C.; Francke, R.; de Haan, R.; Ippel, J. H.; Daalmans, G. J.; Westra Hoekzema, A. J. A.; van Wijk, J. *Magn. Reson. Chem.* **1994**, *32*, 670−678.

(14) Maciel, G. E.; Mclver, J. W., Jr.; Ostlund, N. S.; Pople, J. A. *J. Am. Chem. Soc.* **1970**, *92*, 4497−4506.

(15) (a) Booth, H. *Tetrahedron Lett.* **1965**, 411−416. (b) Sternhell, S. *Quart. Rev.* **1969**, *23*, 236−270.

(16) (a) Bagno, A. *Chem. Eur. J.* **2000**, *6*, 2925−2930. (b) Bagno, A. *Chem. Eur. J.* **2001**, *7*, 1652−1661.

(17) (a) Tähtinen, P.; Bagno, A.; Klika, K. D.; Pihlaja, K. *J. Am. Chem. Soc.* **2003**, *125*, 4609−4618 and references therein. (b) Pihlaja, K.; Tähtinen, P.; Klika, K. D.; Jokela, T.; Salakka, A.; Wähälä, K. *J. Org. Chem.* **2003**, *68*, 6864−6869.

(18) (a) Wolfrom, M. L.; Thompson, A. In *The Carbohydrates*; Pigman, W. W., Ed.; Academic Press: New York, 1957; pp 236−240. (b) Horton, D.; Nakadate, M.; Tronchet, J. M. J. *Carbohydr. Res.* **1968**, *7*, 56−65. (c) Morgenlie, S. *Acta Chem. Scand.* **1973**, *27*, 3609−3610. (d) Jarosz, S.; Krajewski, J. W.; Zamojski, A.; Duddeck, H.; Kaiser, M. *Bull. Pol. Acad. Sci., Chem.* **1985**, *33*, 181−187; *Chem Abstr.* **1986**, *104*, 149270m. (e) Asakura, J.; Matsubara, Y.; Yoshihara, M. *J. Carbohydr. Chem.* **1996**, *15*, 231−239 and references therein. (f) Cao, S.; Hernández-Matéo, F.; Roy, R. *J. Carbohydr. Chem.* **1998**, *17*, 609−631.

(19) (a) Ito, Y.; Ogawa, T. *Tetrahedron Lett.* **1988**, *29*, 1061−1064. (b) Ito, Y.; Ogawa, T.; Numata, M.; Sugimoto, M. *Carbohydr. Res.* **1990**, *202*, 165−175. (c) Kunz, H.; Zimmer, J. *Tetrahedron Lett.* **1993**, *34*, 2907−2910.

(20) Nashed, E. M.; Glaudemans, C. P. J. *J. Org. Chem.* **1987**, *52*, 5255−5260.

(21) Schmidt, O. T. *Methods Carbohydr. Chem.* **1963**, *2*, 318−325.

(22) Banks, M. R.; Blake, J.; Cadogan, J. I. G.; Dawson, I. M.; Gaur, S.; Gosney, I.; Gould, R. O.; Grant, K. J.; Hodgson, K. G. *J. Chem. Soc., Chem. Commun.* **1993**, 1146−1148.

(23) Lorette, N. B.; Howard, W. L.; Brown, J. R., Jr. *J. Org. Chem.* **1959**, *24*, 1731−1733.

(24) (a) Jones, E. R. H.; Meakins, G. D.; Pragnell, J.; Müller, W. E.; Wilkins, A. L. *J. Chem. Soc., Perkin Trans. 1* **1974**, 2376−2380. (b) Greene, T. W.; Wuts, P. G. M. *Protective Groups in Organic Synthesis*, 3rd ed.; Wiley & Sons: New York, 1999; pp 207−215.

propylidene source such as 2,2,-dimethoxypropane.[18e] Many other variations on these themes have also been reported.[3a,18e] In this work, acid-catalyzed derivatization in the presence of $CuSO_4$ was utilized without the use of DMF as a cosolvent at ambient temperature, as this provided the thermodynamically more stable 1,2:3,4-di-*O*-isopropylidene pyranose derivative (**2**) in virtually quantitative yield[18b] in contrast to other conditions[3a,18c] where the 1,2:5,6-di-*O*-isopropylidene furanose derivative was also obtained in significant amounts as a kinetic product. In addition to compounds **2**−**4**, the pentaacetate of **1a** (1,2,3,4,6-penta-*O*-acetyl-α-D-galactopyranose, **5a**) was also prepared using literature methodology for conformational analysis both in solution and in the crystalline form. Its anomer, **5b**, was also examined in the solution state.

The measurement of the ^{1}H and ^{13}C NMR parameters for compounds **1**−**5** followed and the assignments subsequently made using a standard set of correlation experiments (see general experimental details in Supporting Information). Previous evaluations of the coupling constants using the Karplus relationship for comparison to the experimental values have yielded both a poor set of values[5a] and an excellent set,[5b] in both cases purportedly for the same $^{O}S_2$ conformer of **2**. Indeed, for the latter study it seems that due to the higher order of the spectrum, the experimental value for $J_{H4,H5}$ was underestimated (1.3 Hz), and with the better value extracted here (1.95 Hz), it matches the previously calculated value (1.85 Hz) more closely. A third study concluded[18d] a rigid conformation intermediate between $^{O}S_2$ and $B_{2,5}$ to be present. Needless to say, correct assignment of coupling constants and reliable extraction of their magnitude is requisite for correct conformational assessment, which has not always been the case.[5a] Even at the high fields currently available, this is not necessarily trivial in some instances due to severe signal overlap per se or consequential higher order effects precluding manual extraction, and only by resorting to spin simulation/iteration techniques (e.g., the program Perch[25]) could values be reliably extracted. In some cases (e.g., **5a**), this was extremely difficult to do from first principles and changes of solvent were necessary to provide well-separated signals where the $J_{H,H}$s could be reliably extracted and then used as a basis for the solution of the problematic spectra. The ^{1}H and ^{13}C NMR parameters for **1**−**5** obtained under various conditions are listed in Tables 1−3, respectively. Interestingly, a large number of long-range couplings were extractable, particularly from H-1 of the α-anomer independent of the conformation adopted. Moreover, it is difficult to clearly categorize many of these couplings as w-type, sickle,[26] etc.

For both the galactoses **1a** and **1b**, the pyranose ring adopted a $^4C_1$ chair conformation as clearly evidenced by the vicinal couplings involving the ring protons, with the only significant difference being the coupling between H-1 and H-2 due to the differing configuration at position 1. The same was true also for the pentaacetates of **1a** and **1b**. For the glucose moiety of **3**, the observed coupling constants were also fully consistent with the adoption of an ideal $^4C_1$ chair conformation by the glucosyl pyranose ring. However, only very small differences between the conformations adopted by the compounds **2**−**4** were in evidence, as essentially the same vicinal ring coupling constants were observed for all three compounds for the galactose moiety, which is clearly not in an ideal chair $^4C_1$ conformation, or for that matter, in an inversed $^1C_4$ conformation. Thus, neither the glucose group in **3** nor the *tert*-butyldiphenylsilyl group in **4** appeared to influence to any great extent the galactose ring conformation in their respective structures. Thus, it was deemed appropriate to concentrate the analysis on **2** and refer the conclusions drawn to **3** and **4** by analogy. Since substitution at O-6 in the galactose ring for compounds **2**−**4** has only a negligible effect on the galactose ring conformation, it is therefore the isopropylidene groups that are determinant for the galactose ring conformation in these compounds.

Of all the skew and boat conformations that are possible for a galactose ring (six distinct conformers for each category), inspection of the structures permitted the immediate elimination of three conformers, $^{1,4}B$, $B_{1,4}$, and $^1S_3$, on the basis of the geometrical constraints of the isopropylidene groups. For these three structures, the two isopropylidene groups would both be attached to the galactose ring via an axial and an equatorial linkage, which is considered unfavorable in comparison to the other nine structures where at least one isopropylidene group is attached favorably, either by two axial, two equatorial, axial and *cis*-isoclinal, or equatorial and *cis*-isoclinal linkages. The standout conformation is the $^{O}S_2$ conformation where both isopropylidene groups are attached by an axial and a *cis*-isoclinal linkage, and clearly this conformer should be the most favored. But the problem of distinguishing between a confluence of contributing conformers (i.e., a time-averaged spectrum of several conformers), where the number of permutations involving up to nine structures abound, and a system that is conformationally biased can be simplified if the expected coupling constant values based on the dihedral angles are too divergent from the observed coupling constants for the vicinal ring protons and used as a basis for eliminating that conformer. That is to say, if a particular coupling constant from the set of coupling constants for one conformer is expected to have a very large coupling in contrast to that observed (and conversely), then that conformer can be eliminated. On this basis, six more conformers were eliminated as likely contributing candidate structures, leaving only three candidates: the $^{O}S_2$, $^1S_5$, and $B_{2,5}$ conformers (depicted for **1a** in Scheme 2), although the boat conformation is considered to be an unlikely contributor on energetic grounds.

It was important to limit the number of candidate structures to maintain a reasonable, and affordable, set of structures for the calculations. The problem of still distinguishing between a conformational equilibrium, even one that is heavily biased, and the total predominance of one conformer can be accomplished if the calculations can predict energetically either system and the calculated coupling constants (population-weighted in the case of a conformational equilibrium) match the

(25) See, for example: Laatikainen, R.; Niemitz, M.; Weber, U.; Sundelin, J.; Hassinen, T.; Vepsäläinen, J. *J. Magn. Reson., Ser. A* **1996**, *120*, 1−10. See also Peak Research NMR Software; Perch Solutions, Ltd.: Kuopio, Finland, 2003 (website: http://www.perchsolutions.com).

(26) Mark, V. *Tetrahedron Lett.* **1974**, *15*, 299−302.

TABLE 1. ^{1}H Chemical Shifts (ppm) and Multiplicities for Compounds 1−5 at 25 °C[a]

	H-1	H-2	H-3	H-4	H-5	H-6$_A$[b]	H-6$_B$[b]	H-8	H-9	H-10	H-11	H-12	H-14	H-16
1a[c]	5.266, d	3.808, d_{AB}d	3.855, d_{AB}d	3.988, ddd	4.091, dist dddd	3.741, ho mult	3.728, ho mult							
1b[c]	4.586, d	3.494, d_{AB}dd	3.648, d_{AB}d	3.930, dist ddd	3.710, $d_{AB}d_{AB}$d	3.772, $d_{AB}d_{AB}$	3.747, ovld							
2[d,e]	5.563, d	4.336, dd	4.617, dd	4.280, app dd	3.876, d_{AB}dd	3.827,[b] $d_{AB}d_{AB}$	3.729,[b] br d_{AB}d	1.337, qt	1.536, br s		1.341, qt	1.454, qt		
2[f,g]	5.461, d	4.321, ovld dd	4.604, dd	4.308, ovld dd	3.834, dist td	3.649, $d_{AB}d_{AB}$	3.607, $d_{AB}d_{AB}$	1.312, qt	1.467, br s		1.307, qt	1.363, qt		
2[f,h]	5.498, d	4.427, dd	4.683, dd	4.335, dd	3.813, dist td	3.56−3.67, complex ovld mult		1.327, br s	1.474, br s		1.319, br s	1.358, br s		
2[f,i]	5.510, d	4.471, dd	4.715, dd	4.349, dist dd	3.814, td (br)	3.56−3.67, complex ovld mult		1.333, br s	1.478, br s		1.326, br s	1.358, br s		
2[j]	5.419, d	4.296, dd	4.554, dd	4.217, dd	3.700, ddd	3.471, ddd	3.394, ddd	1.265, br	1.428, s		1.319, s	1.261, br		
2[k]	5.452, d	4.139, dd	4.421, dd	3.941, dd	3.934, ddd	3.904, dd	3.752, dd	1.106, s	1.450, s		1.171, s	1.425, s		
3[d] (galactose part)	5.103, d	4.095, dd	4.400, dd	3.994, dist dd	3.679, ovld	3.940, ho mult	3.695, ovld	1.022, dist qt	1.028, dist mult		1.233, qt	1.393, qt		
3[d,l] (glucose part)	5.448, d	4.314, dd	5.844, dd	5.164, dd	3.888, ddd	4.344, d_{AB}d	4.168, d_{AB}d	1.859,[m] s	2.028,[m] s		2.113,[m] s			
4[d,n]	5.509, d	4.292, dd	4.603, dd	4.351, dd	3.931, $d_{AB}d_{AB}$d	3.869, $d_{AB}d_{AB}$	3.819, $d_{AB}d_{AB}$	1.331, qt	1.518, br s		1.335, qt	1.396, qt		
5a[d]	6.382, ho mult	5.338, ho mult	5.343, ho mult	5.505, ho mult	4.348, dist tdd	4.117, d_{AB}d	4.090, d_{AB}d	2.165, s		2.009, s		2.025, s	2.163, s	2.046, s
5a[f]	6.325, dqt	5.226, d_{AB}dd	5.354, $d_{AB}d_{AB}$d	5.511, ddt	4.520, tdd	4.125, d_{AB}d	4.058, d_{AB}d	2.162, s		1.996, s		1.956, s	2.151, s	1.976, s
5b[d]	5.703, d	5.339, dist ddd	5.083, dd	5.430, ddd	4.057, $d_{AB}d_{AB}$d	4.163, $d_{AB}d_{AB}$	4.128, $d_{AB}d_{AB}$	2.126, s		2.048, s		1.998, s	2.169, s	2.047, s

[a] Legend: AB, not quite 1st order, line intensities perturbed; app, apparent; apr, approximate; br, broad; dist, distorted; d, doublet; ho, higher order; mult, multiplet; nc, not calculated; ne, not extracted by Perch; obs, obscured; ovld, overlapped; qt, quartet; s, singlet; sl, slightly; t, triplet; v, very. [b] H-6s were not assigned and are distinguished simply on the basis of their chemical shifts (the more downfield signal is denoted by a subscript A, etc.). H-6s were assigned for compound **2** in ref 5b, and on this basis, the more downfield H-6 proton at 3.827 ppm is H-6*pro-R* (H-6$_A$) and the more upfield H-6 proton resonating at 3.729 ppm is H-6*pro-S* (H-6$_B$). [c] In D_2O referenced to TSP (0 ppm). The data for **1a** were extracted from a spectrum acquired on a freshly prepared sample of **1a** that essentially contained only **1a** (i.e., α-D-galactopyranose). The data for **1b** were extracted from a spectrum acquired on an equilibrated sample containing *β*-D-galactopyranose and α-D-galactopyranose (2.02:1, respectively) in addition to minor amounts of furanose and open-chain forms, but despite considerable spectral overlap, the values are nonetheless reported with confidence. [d] In $CDCl_3$ referenced to TMS (0 ppm). [e] Signal for HO-6 was normally observed in the range 2.2−2.7 ppm; for this particular sample, it resonated at 2.634 ppm as a very broad singlet. [f] In acetone-d_6 referenced to TMS (0 ppm). [g] At 25 °C; HO-6 not observed. [h] At −75 °C; for HO-6: 4.551, app dd. [i] At −100 °C; for HO-6: 4.794, dist app dd. [j] In DMSO-d_6 referenced to DMSO-d_5 (2.49 ppm). A signal for HO-6 was observed at 4.665 ppm (dd, $J_{H6_A} = 6.60$, $J_{H6_B} = 5.04$ Hz). [k] In toluene-d_8 referenced to toluene-d_7 (2.09 ppm). [l] For the phthalimido moiety: 7.839 (v br AA′ portion of an AA′BB′ system mult, $J_{H10'} = 7.55$ and |0.95| Hz, $J_{H9'}$ ne, H-9′); 7.714 (BB′ portion of an AA′BB′ system mult, $J_{H9'} = 7.55$ and |0.95|, $J_{H10'} = 7.55$ Hz, H-10′). [m] Protons H-12′, H-14′, and H-16′, respectively. [n] For the TBDPS group: 7.704 (ovld mult, $J_{H15_A} = 7.45$ and |0.70|, $J_{H16_A} = |1.37|$, $J_{H14_A} = |1.29|$ Hz, H-14$_A$); 7.680 (ovld mult, $J_{H15_B} = 7.45$ and |0.70|, $J_{H16_B} = |1.37|$, $J_{H14_B} = |1.28|$ Hz, H-14$_B$); 7.4021 (ovld mult, $J_{H15_A} = 7.47$, $J_{H14_A} = |1.37|$ Hz, H-16$_A$); 7.4018 (ovld mult, $J_{H15_B} = 7.49$, $J_{H14_B} = |1.37|$ Hz, H-16$_B$); 7.359 (ovld mult, $J_{H16_B} = 7.49$, $J_{H14_B} = 7.45$ and |0.70|, $J_{H15_B} = |1.27|$ Hz, H-15$_B$); 7.355 (ovld mult, $J_{H16_A} = 7.47$, $J_{H14_A} = 7.45$ and |0.70|, $J_{H15_A} = |1.27|$ Hz, H-15$_A$); 1.062 (s, H-18).

TABLE 2. Experimental and Calculated Vicinal, Geminal, and Long-Range $J_{H,H}$s (Hz) for Compounds 1−5 at 25 °C[a]

compd	source[b]	conf	$J_{H1,H2}$	$J_{H2,H3}$	$J_{H3,H4}$	$J_{H4,H5}$	$J_{H5,H6_A}$	$J_{H5,H6_B}$	$J_{H6_A,H6_B}$[c]	$J_{H1,H3}$	$J_{H1,H4}$	$J_{H1,H5}$	$J_{H1,H9}$	$J_{H2,H4}$	$J_{H8,H9}$	$J_{H11,H12}$
1a[d]	exp	$^4C_1$	3.97	10.33	3.42	1.23	4.47	7.96	−11.61	−0.43[e]	0.51[e]	−0.59[e]		−0.37[e]		
1a	DFT (ex **5a**)	$^4C_1$	3.44	9.11	4.20	2.59	nc	nc	nc	−0.37	0.65	−0.70		−0.54		
1a	DFT (man)	$^4C_1$	4.03	8.85	3.53	1.66	nc	nc	nc	nc	0.73	nc		−0.54		
1a	DFT (ex **3**)	$^OS_2$	4.20	4.46	6.66	3.86	nc	nc	nc	nc	0.14	nc		−0.54		
1b[d]	exp	$^4C_1$	7.93	9.95	3.51	1.11	7.90	4.44	−11.68	ne	ne	ne		−0.40[e]		
2[f,g]	exp	$^OS_2$	5.04	2.42	7.94	1.95	7.15	4.61	−11.65	<|0.2|	ne	−0.59[e]	0.36[c]	ne	−0.76[c]	−0.71[c]
2[h,i]	exp	$^OS_2$	5.04	2.34	7.97	1.89	5.86	6.47	−10.81	−0.24[e]	0.30[e]	−0.53[e]	0.32[c]	−0.17[e]	−0.64[c]	−0.61[c]
2[h,j]	exp	$^OS_2$	5.06	2.30	8.04	1.74	6.54	6.48	ne	ne	0.25[e]	−0.56[e]	ne	ne	ne	ne
2[h,k]	exp	$^OS_2$	4.97	2.29	8.01	1.80	6.28	6.57	ne	ne	ne	ne	ne	ne	ne	ne
2	X-ray (ex **3**)	$^OS_2$	4.96	2.59	7.33	2.26	nc	nc	nc	nc	0.31	nc	nc	−0.20	nc	nc
2	DFT (ex **3**)	$^OS_2$	4.79	3.19	7.25	2.26	nc	nc	nc	nc	0.31	nc	nc	−0.28	nc	nc
2	Karplus	$^OS_2$	4.77	2.62	7.87	1.85	8.10	4.65	nc	nc	nc	nc	nc	nc	nc	nc
2[l]	exp	$^OS_2$	5.04	2.26	7.99	1.84	6.36	6.56	−10.92	ne	ne	ne	ne	ne	ne	ne
2[m]	exp	$^OS_2$	5.03	2.38	7.86	1.79	7.21	4.76	−11.48	ne	ne	ne	ne	ne	ne	ne
3[f,n]	exp	$^OS_2$	5.09	2.42	7.91	1.83	3.61	8.13	−11.96	−0.27[e]	0.32[e]	−0.54[e]	0.20[c]	−0.16[e]	−0.57[c]	−0.62[c]
3[f,o]	exp	$^4C_1$	8.51	10.69	9.06	10.18	4.56	2.32	−12.23	ne	ne	ne		ne		
4[f]	exp	$^OS_2$	4.99	2.32	7.97	1.84	7.11	6.25	−10.02	−0.24[e]	ne	−0.57[e]	0.29[c]	ne	−0.64[c]	−0.60[c]
5a[f]	exp	$^4C_1$	3.69	10.94	3.38	1.44	6.94	6.53	−11.33	−0.46[e]	0.48[e]	−0.63[e]		−0.53[e]		
5a[h]	exp	$^4C_1$	3.72	10.93	3.42	1.46	6.57	6.54	−11.27	−0.44[e]	0.49[e]	−0.63[e]		−0.41[e]		
5a	X-ray	$^4C_1$	4.46	8.94	3.27	1.75	nc	nc	nc	−0.37	0.56	−0.62		−0.37		
5a	DFT	$^4C_1$	3.69	11.48	3.69	1.83	nc	nc	nc	−0.45	0.56	−0.70		−0.45		
5b[f]	exp	$^4C_1$	8.33	10.43	3.44	1.23	6.70	6.59	−11.36	ne	ne	ne		−0.39[e]		

[a] Legend: nc, not calculated; ne, not extracted by Perch. [b] Experimental values are indicated by exp. X-ray indicates that the X-ray structure was imported into *Gaussian 98W* for calculation of the $J_{H,H}$s (i.e., geometry optimization was not performed, but one SCF cycle was run). DFT indicates geometry-optimized structures starting either from the X-ray structure (structure origin is given) or from a structure that was drawn free-hand and preoptimized by MM2 prior to optimization by DFT (man). In the case of **1a**, two different $^4C_1$ conformers were obtained (differing mainly in the disposition of the ring substituents rather than the ring conformation itself) depending on the starting structure. Karplus indicates that the couplings were calculated using this relationship (from ref 5b). [c] Sign of J was assumed (^{even}J = −ve, ^{odd}J = +ve). [d] In D_2O. The data for **1a** were extracted from a spectrum acquired on a freshly prepared sample of **1a** that essentially contained only **1a** (i.e., α-D-galactopyranose). The data for **1b** were extracted from a spectrum acquired on an equilibrated sample containing β-D-galactopyranose and α-D-galactopyranose (2.02:1, respectively) in addition to minor amounts of furanose and open-chain forms, but despite considerable spectral overlap, the values are nonetheless reported with confidence. [e] Sign of J was taken from the DFT calculations. [f] In $CDCl_3$. [g] In some samples, $J_{HO6,H6_B}$ could occasionally be observed (ca. 6.4 Hz). [h] In acetone-d_6. [i] At 25 °C. A value for $J_{H3,H6_A}$ (0.36[b] Hz) was also extracted. [j] At −75 °C. These values are reported as they are the lowest temperature at which the field homogeneity was still good (ν_{tms} = 0.5 Hz). Coupling between HO-6 and the two H-6s could be observed at this temperature, but due to the complexity of the spectral region containing the H-6s (an overlapped mass consisting of two sets of higher order spin pairs), $J_{HO6,H6_A}$, $J_{HO6,H6_B}$, and $J_{H6_A,H6_B}$ could not be reliably extracted. [k] At −100 °C. Although the field homogeneity had deteriorated (ν_{tms} 1 = Hz), the values reported are still considered to be reliable. As at −75 °C, the full spin system could not be accurately simulated. [l] In DMSO-d_6.[m] In toluene-d_8. [n] Coupling constants for the galactose ring of **3**. [o] Coupling constants for the glucose ring of **3**.

TABLE 3. ^{13}C Chemical Shifts (ppm) for Compounds 1−5 at 25 °C

	C-1	C-2	C-3	C-4	C-5	C-6	C-7	C-8	C-9	C-10	C-11	C-12	C-13	C-14	C-15	C-16
1a[a]	95.11	71.18	72.01	72.14	73.31	64.02										
1b[a]	99.29	74.72	75.63	71.58	77.98	63.82										
2[b]	96.29	70.58	70.74	71.47	68.25	62.10	108.67	24.95	26.02	109.42	24.34	25.93				
2[c,d]	97.21	71.58	71.60	71.81	69.49	61.83[e]	108.84	25.18	26.32	109.42	24.59	26.38				
2[c,f]	96.47	70.28	70.33	70.45	68.52[g]	60.77[h]	108.33	24.61	25.67	108.47	23.46	25.67				
2[i]	95.61	69.95	69.95	70.10	68.19	59.92	107.60	24.86	25.92	108.01	24.19	25.83				
2[j]	95.70	70.12	70.23	70.56	68.19	61.14	107.48	23.85	25.13	108.22	23.32	25.10				
3,[b] gal	95.92	70.15	70.65	70.88	67.48	69.41	107.98	24.65	25.34	109.31	24.24	25.88				
3,[b,k] glu	99.38	54.58	70.71	69.06	71.59	62.07	170.10[l]	20.47[l]	169.54[l]	20.65[l]	170.74[l]	20.78[l]				
4[b,m]	96.30	70.90	70.62	70.68	68.34	62.60	108.43	24.99	26.10	109.00	24.39	25.96				
5a[b]	89.72	67.37	66.45	67.43	68.77	61.26	169.06	21.03	170.26	20.80	170.02	20.75	170.29	20.68	170.50	20.78
5a[c]	90.08	67.44	68.05	68.41	69.62	61.92	169.62	20.39	170.44	20.66	170.21	20.49	170.65	20.46	170.44	20.49
5b[b]	92.19	67.88	70.86	66.84	71.74	61.06	168.97	20.97	169.38	20.70	169.96	20.78	170.13	20.81	170.35	20.81

[a] In D_2O referenced to TSP (0 ppm). The data for **1a** were extracted from a spectrum acquired on a freshly prepared sample of **1a** that essentially contained only **1a** (i.e., α-D-galactopyranose). The data for **1b** were extracted from a spectrum acquired on an equilibrated sample containing β-D-galactopyranose and α-D-galactopyranose (2.02:1, respectively) in addition to minor amounts of furanose and open-chain forms. [b] In $CDCl_3$ referenced to TMS (0 ppm). [c] In acetone-d_6 referenced to TMS (0 ppm). [d] At 25 °C. [e] Major signal (br), minor signal 61.7 (ex br). [f] At −100 °C. [g] Major signal, minor signal 68.49 (integration, 5:3). [h] Major signal, minor signal 60.64. [i] In DMSO-d_6 referenced to DMSO-d_5 (39.5 ppm). [j] In toluene-d_8 referenced to toluene-d_7 (20.4 ppm). [k] For the phthalimido moiety: 167.63 (v br, C-7′); 133.74 (C-10′); 132.01 (v br, C-8′); 123.48 (C-9′). [l] Carbons C-11′−C-16′, respectively. [m] For the TBDPS group: 135.71 (C-14_A); 135.64 (C-14_B); 133.68 (C-13_B); 133.64 (C-13_A); 129.57 (C-16_B); 129.56 (C-16_A); 127.59 (C-15_B); 127.54 (C-15_A); 26.83 (C-18); 19.28 (C-17).

experimental values. However, if a conformational equilibrium is in effect, then examination of the system by variable-temperature NMR will reveal the presence of such, either by, in the best case scenario, slowing the interconversion rate sufficiently on the NMR-time scale to permit explicit observation of the subspectra of each of the contributing conformers or, in less than ideal cases, by perturbation of the spectra in some manner. Compound **2** was thus cooled to −100 °C with spectra recorded in acetone-d_6 at intervals of 25 °C (results for spectra at 25, −75, and −100 °C included in Tables 1−3). However, immediate interpretation was compromised by the re-

SCHEME 2

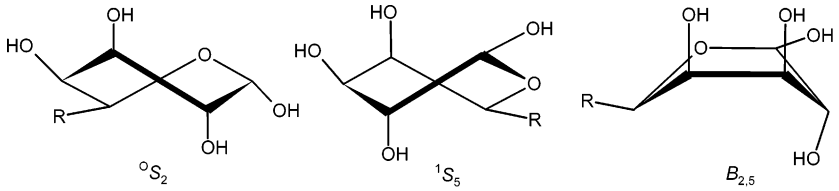

stricted rotation about the C_5-C_6 bond; this was readily attributable by the splitting of C-6 already at 25 °C, followed subsequently by C-5, which decoalesced at −75 °C into the same 5:3 ratio of conformer signals. Of **2**−**4**, only for **2** and only in acetone-d_6 were the dynamic effects of the C_5-C_6 restricted bond rotation evident at ambient temperature. For both C-5 and C-6, a barely perceptible broadening continued after decoalescence, indicating that an additional species was present but was still in fast exchange with the two, now observable conformers. This additional species is presumably the third rotamer for rotation about the C_5-C_6 bond, as has been previously described.[5b] This dynamic process affects the entire system, although the effects are generally most notable for the nuclei close to the point of action (hence the basis for the assignment). Thus, all proton signals, with the exception of H-1, showed varying degrees of modest to slight broadening, including even the methyl signals. Although the H-6s are close to the point of action and therefore highly subject to change, comprehension of their behavior was compounded by the slowing of the chemical exchange of HO-6, which not only became observable with the decrease in temperature but in fact displayed coupling to the H-6s, rendering their spin simulation prohibitive. In the ^{13}C NMR, aside from the decoalescence of C-5 and C-6, most signals displayed some degree of broadening due to exchange, although none were dramatically broadened. So although the dynamics of the C_5-C_6 bond can influence the band shapes of practically all of the observed nuclei in the molecule, this is a consequence of the differing chemical shifts of each of the nuclei in the various rotamers. However, it is unlikely that the dynamics of the C_5-C_6 bond can influence the coupling constants of the vicinal ring protons to any large degree. Therefore, if a conformational equilibrium was in effect, while the band shape changes may be masked by the other dynamic process, any changes in the vicinal coupling constants for the ring protons should be apparent and, moreover, decisive. Extraction of the coupling constants at both −75 and −100 °C for **2** revealed that essentially no change whatsoever was evident for the determinant vicinal couplings. Therefore, on the basis of this low-temperature experiment, the system is concluded to be overwhelmingly dominated by one conformer in the solution state and it remains only to distinguish between the $^{O}S_2$ and $^{1}S_5$ conformers.

Single-crystal X-ray analyses were also performed on **3** and **5a** enabling a comparison between the conformations adopted in the crystalline state and in solution. Compound **3** crystallized in the hexagonal crystal system, space group $\mathscr{P}65$, while **5a** crystallized in the orthorhombic crystal system, space group $\mathscr{P}2_12_12_1$. The crystal structures of both compounds showed normal structural bonding parameters; however, there was some degree of disorder for **3** as the C_6-acetyl group fragment could assume one of two orientations, one of which is depicted in Figure 1 (the ORTEP plots of both **3** and **5a** are presented in Supporting Information, Figures S1 and S2, respectively). For **3**, an $^{O}S_2$ conformation was found for the galactose moiety in the crystalline state. By comparison, a $^{4}C_1$ conformation was still adopted by **5a** (and also for the glucose moiety in **3**), i.e., peracetylation did not alter the preferred conformation from α-D-galactopyranose (**1a**). Of note in **3** is the torsion angle defined by $H_2-C_2-C_3-H_3$, which is larger than the $H_4-C_4-C_5-H_5$ torsion angle (72 vs 46°, respectively), yet the magnitude of the proton coupling in the former set is greater (2.42 vs 1.83 Hz, respectively).

The X-ray structure coordinates of **3** and **5a** were imported directly into *Gaussian 98W*.[27] To limit the length of the calculations, the glucosyl moiety attached to O-6 in **3** was substituted by H, thereby generating structure **2**. DFT calculations (perturbations on a particular nucleus) at the B3LYP/cc-pVTZ level of theory were performed in order to calculate the couplings emanating from the selected proton. (H-2 and H-4 in all cases (**1a**, **2**, and **5a**), thereby obtaining all vicinal $^1H-^1H$ couplings of the sugar ring and additionally H-1 for **1a** and **5a** to obtain long-range couplings involving H-1.) The coupling constant calculations are based on the assumption that the Fermi contact term dominates the coupling and the other contributions are either insignificant (spin−dipole term) or cancel each other out (paramagnetic and diamagnetic spin−orbit terms).[16,17] The results of the calculations are also presented in Table 2.

In this approach, by using the X-ray structures unaltered (except the substitution and with one SCF cycle run on the geometries to set the electron distributions), good agreement was obtained with respect to the experimental values for both **2** and **5a** (including $J_{H2,H3}$ and $J_{H4,H5}$). The X-ray-based structures were also used as initial structures for geometry optimization (at the B3LYP/6-31G(d,p) level of theory) to provide a further comparison; very similar results were obtained, thus validating the use of the unaltered X-ray structures and further confirming that the conformation of the galactose ring in solution is indeed dominated, overwhelming so, by the $^{O}S_2$ conformation for **2**−**4**. The two geometry-

(27) Frisch, M. J.; Trucks, G. W.; Schlegel, H. B.; Scuseria, G. E.; Robb, M. A.; Cheeseman, J. R.; Zakrzewski, V. G.; Montgomery, J. A., Jr.; Stratmann, R. E.; Burant, J. C.; Dapprich, S.; Millam, J. M.; Daniels, A. D.; Kudin, K. N.; Strain, M. C.; Farkas, O.; Tomasi, J.; Barone, V.; Cossi, M.; Cammi, R.; Mennucci, B.; Pomelli, C.; Adamo, C.; Clifford, S.; Ochterski, J.; Petersson, G. A.; Ayala, P. Y.; Cui, Q.; Morokuma, K.; Malick, D. K.; Rabuck, A. D.; Raghavachari, K.; Foresman, J. B.; Cioslowski, J.; Ortiz, J. V.; Stefanov, B. B.; Liu, G.; Liashenko, A.; Piskorz, P.; Komaromi, I.; Gomperts, R.; Martin, R. L.; Fox, D. J.; Keith, T.; Al-Laham, M. A.; Peng, C. Y.; Nanayakkara, A.; Gonzalez, C.; Challacombe, M.; Gill, P. M. W.; Johnson, B. G.; Chen, W.; Wong, M. W.; Andres, J. L.; Head-Gordon, M.; Replogle, E. S.; Pople, J. A. *Gaussian 98*, revision A.11; Gaussian, Inc.: Pittsburgh, PA, 2001.

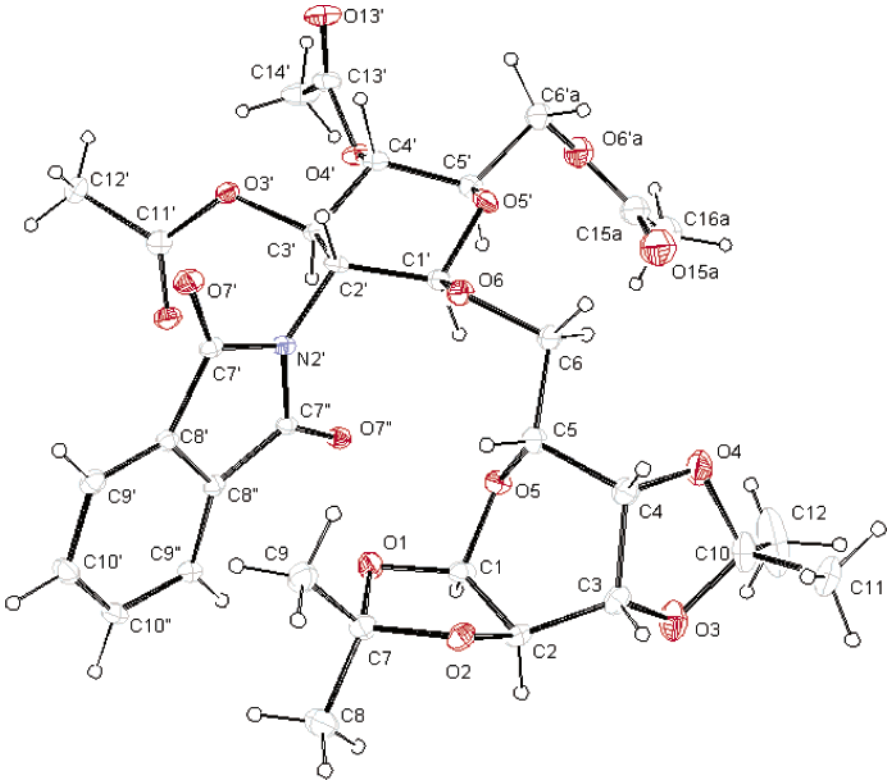

FIGURE 1. Structure of the disaccharide **3** as determined by X-ray analysis. The thermal displacement parameters are drawn at 20% probability.

optimized structures were also used as the starting geometries for α-D-galactose (**1a**) after replacement of the *O*-bound substituents with H. The structure for **1a** with an $^{O}S_2$ conformation maintained its general shape but provided values, not unexpectedly, inconsistent with the observed values in contrast to the $^4C_1$ conformation (e.g., **5a**), which provided very consistent values. Two other structures were also input for geometry optimization. One was a manually generated $^1S_5$ conformer for **2** (on the basis that it should also provide couplings similar to those observed) but which only resulted in the same, indistinguishable $^{O}S_2$ conformer being obtained as that resulting from the optimization of the X-ray-based structure. This result infers that the $^1S_5$ conformation does not represent a local energy minimum on the PES and is thus not expected to participate as a discrete entity to any conformational equilibrium. The other input structure was a manually generated $^4C_1$ conformation for **1a**. Differences were apparent between this $^4C_1$ conformation and the $^4C_1$ conformation provided by DFT optimization of the X-ray-based structure, but the differences reside mainly in the disposition of the ring substituents rather than any differences in the ring conformation and reflect the effects that the attendant substituent orientations can have on the coupling constants. Of note, in the cases where long-range coupling constants were able to be extracted, the DFT calculations provided remarkably accurate values. These coupling constants in themselves speak for a conformationally biased system, particularly when the DFT calculations have been able to reproduce them so faithfully.

Conclusion

In conclusion, the NMR parameters of **1**−**5**, despite the long prevalence of some of the compounds in the literature, have not always been properly reported, mainly due to difficulties associated with overlap and higher order. The conformation of the diisopropylidene derivatives of galactose (**2**−**4**), despite having been examined previously, nevertheless represented a good test case for the recent developments[16] that have been made in the calculation of $J_{H,H}$ using DFT methodology and which is now proving to be a useful structural tool.[17] The calculation of only coupling constants and not chemical shifts, despite the economical superiority of the latter, for the conformational determination was based on previous work[17a] where the calculation of δ_Hs was shown to be inadequate and inferior to the use of $J_{H,H}$s for this type of analysis. A different approach was also tried by using the structures of two of these compounds, **3** and **5a**, resulting from X-ray analysis directly for the calculation of the vicinal coupling constants; it was found that they not only were appropriate as is but also provided good starting structures for further refinement. Thus the work, based on a combination of X-ray analysis, molecular modeling, and NMR, has confirmed the overwhelming conformational bias of **2**−**4** toward an $^{O}S_2$ conformation both in solution and in the crystalline state. The demonstrated[28] efficacy of DFT calculations in evaluating long-range couplings in saccharides is valuable for distinguishing between hydrogen bond-mediated pathways

(28) Larsson, E. A.; Ulicny, J.; Laaksonen, A.; Widmalm, G. *Org. Lett.* **2002**, *4*, 1831−1834.

and otherwise normal w-type coupling pathways; differentiation is important, as erroneous structural interpretations can be based on these observations.[28] Evaluation even in small molecules such as those studied here can nevertheless serve well to model larger systems. What was further pertinent was the differences calculated for the two optimized $^4C_1$ conformations of **1a**, demonstrating that there can be realizable differentiation due to substituent orientation.

Acknowledgment. The authors wish to thank Mr. Markku Reunanen for the EIMS measurements. The assistance of Prof. Alessandro Bagno (Università di Padova), whose advice and guidance with the computational work has been most influential, is also gratefully acknowledged. The authors also thank the Center for Scientific Computing (CSC, Finland) for a generous allocation of computation time.

Supporting Information Available: Crystallographic data have been deposited with the Cambridge Crystallographic Data Centre as supplementary publication nos. CCDC-218904 (**3**) and CCDC-218905 (**5a**), copies of which can be obtained upon request from the Director, CCDC, 12 Union Road, Cambridge CB12 1E2, U.K. Computational methodology (essentially the same as that used previously),[17] general experimental details, preparative procedures for compounds **2**−**5a**, and X-ray crystallographic data (including CIF files, structure tables, and XYZ files) for **3** and **5a**. This material is available free of charge via the Internet at http://pubs.acs.org.

JO035400U